

## Article

# A CeO<sub>2</sub>/ZrO<sub>2</sub>-TiO<sub>2</sub> Catalyst for the Selective Catalytic Reduction of NO<sub>x</sub> with NH<sub>3</sub>

Wenpo Shan <sup>1,2</sup>, Yang Geng <sup>3</sup>, Yan Zhang <sup>1,2</sup>, Zhihua Lian <sup>1</sup> and Hong He <sup>1,2,4,\*</sup>
<sup>1</sup> Center for Excellence in Regional Atmospheric Environment, Institute of Urban Environment, Chinese Academy of Sciences, Xiamen 361021, China; wpshan@iue.ac.cn (W.S.); yzhang3@iue.ac.cn (Y.Z.); zhlian@iue.ac.cn (Z.L.)

<sup>2</sup> Ningbo Urban Environment Observation and Research Station-NUEORS, Institute of Urban Environment, Chinese Academy of Sciences, Ningbo 315800, China

<sup>3</sup> School of Environmental and Biological Engineering, Nanjing University of Science and Technology, Nanjing 210094, China; yanggeng\_njust@163.com

<sup>4</sup> State Key Joint Laboratory of Environment Simulation and Pollution Control, Research Center for Eco-Environmental Sciences, Chinese Academy of Sciences, Beijing 100085, China

\* Correspondence: honghe@rcees.ac.cn; Tel./Fax: +86-10-62849123

Received: 30 September 2018; Accepted: 27 November 2018; Published: 30 November 2018



**Abstract:** In this study, CeZr<sub>0.5</sub>Ti<sub>a</sub>O<sub>x</sub> (with a = 0, 1, 2, 5, 10) catalysts were prepared by a stepwise precipitation approach for the selective catalytic reduction of NO<sub>x</sub> with NH<sub>3</sub>. When Ti was added, all of the Ce-Zr-Ti oxide catalysts showed much better catalytic performances than the CeZr<sub>0.5</sub>O<sub>x</sub>. Particularly, the CeZr<sub>0.5</sub>Ti<sub>2</sub>O<sub>x</sub> catalyst showed excellent activity for broad temperature range under high space velocity condition. Through the control of pH value and precipitation time during preparation, the function of the CeZr<sub>0.5</sub>Ti<sub>2</sub>O<sub>x</sub> catalyst could be controlled and the structure with highly dispersed CeO<sub>2</sub> (with redox functions) on the surface of ZrO<sub>2</sub>-TiO<sub>2</sub> (with acidic functions) could be obtained. Characterizations revealed that the superior catalytic performance of the catalyst is associated with its outstanding redox properties and adsorption/activation functions for the reactants.

**Keywords:** Ce-based catalyst; stepwise precipitation; selective catalytic reduction; diesel exhaust; nitrogen oxides abatement

## 1. Introduction

NO<sub>x</sub> (mainly NO and NO<sub>2</sub>) in the atmosphere plays critical roles in the formation of severe air pollution problems, such as haze, acid rain, and photochemical smog. In the last few decades, great efforts have been devoted to the development of NO<sub>x</sub> emission control technologies [1–3]. Selective catalytic reduction of NO<sub>x</sub> with NH<sub>3</sub> (NH<sub>3</sub>-SCR) has been widely applied for the removal of NO<sub>x</sub> generated from stationary sources for many years, and it has also been used for the control of NO<sub>x</sub> emission from diesel vehicles [2,4].

Catalysts play an important role in the development of NH<sub>3</sub>-SCR technology [5,6]. Vanadium-based catalyst (especially V<sub>2</sub>O<sub>5</sub>-WO<sub>3</sub>/TiO<sub>2</sub>), with excellent SO<sub>2</sub> resistance, is the most widely used NH<sub>3</sub>-SCR catalyst for NO<sub>x</sub> emission control from power plants, and it was also applied on diesel vehicles as the first generation of SCR catalyst [4]. However, this catalyst system still has some problems, including the toxicity of active V<sub>2</sub>O<sub>5</sub>, narrow temperature window, and low thermal stability [2].

There has been strong interest in developing a vanadium-free catalyst that can be used on diesel vehicles [5–11]. Ce is a key component in three-way catalysts for emission control in automobiles for gasoline. CeO<sub>2</sub> provides an oxygen storage function through redox cycling between Ce<sup>3+</sup> and

$\text{Ce}^{4+}$ . In recent years, Ce has also attracted great attention for applications as a support [12,13], promoter [14–18], or main active component [19–26] for  $\text{NH}_3$ -SCR catalysts.

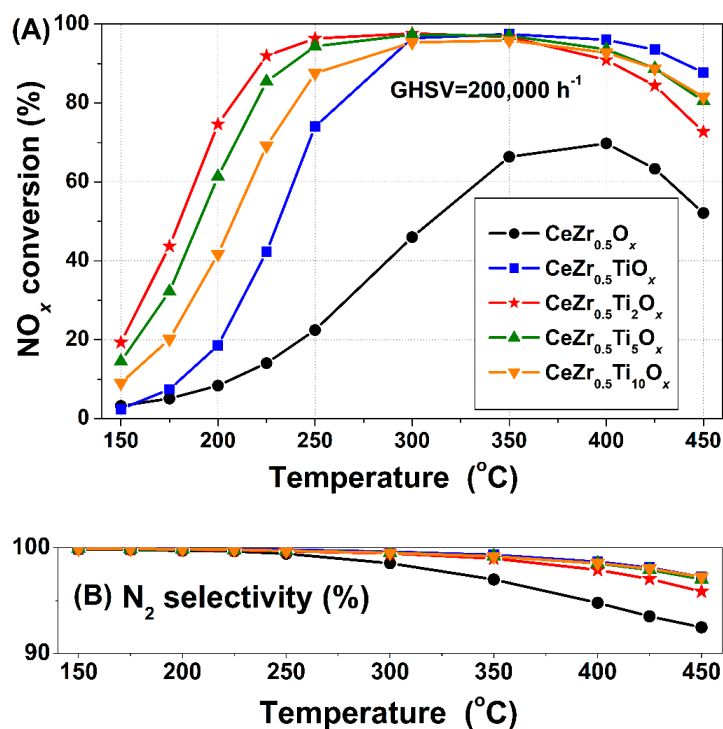
Pure Ce oxide is not suitable for use as an  $\text{NH}_3$ -SCR catalyst [27,28]. When Zr oxide was introduced into Ce oxide, the thermal stability and the oxygen storage capacity of the oxide could be significantly improved. Therefore, Ce-Zr oxide was investigated for  $\text{NH}_3$ -SCR [12,13,29–34]. In the  $\text{NH}_3$ -SCR reaction, both redox functions and acidic functions of the catalyst are needed [4,35]. Therefore, a high dispersion of active sites and close coupling of redox with acid sites is the way to design a highly efficient  $\text{NH}_3$ -SCR catalyst.

In this study, starting from a preparation of Ce-Zr oxide by the co-preparation method, we developed a Ce-Zr-Ti oxide catalyst using a stepwise precipitation approach, under the theoretical guidance of the close combination of the Ce-Zr oxide with strong redox functions and Ti oxide with excellent acid properties [4,5]. This obtained catalyst showed superior catalytic performance for  $\text{NH}_3$ -SCR.

## 2. Results and Discussion

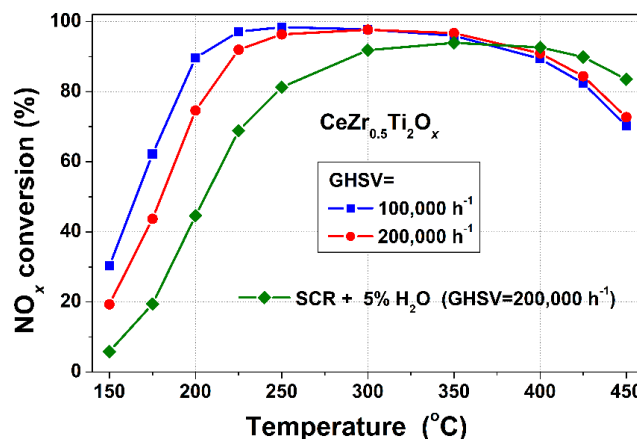
### 2.1. $\text{NH}_3$ -SCR Activity

Figure 1A presents the  $\text{NO}_x$  conversion over the catalysts with different Ti contents under a relatively high gas hourly space velocity (GHSV) of  $200,000 \text{ h}^{-1}$ . The  $\text{CeZr}_{0.5}\text{O}_x$  just exhibited over 50%  $\text{NO}_x$  conversion in a narrow temperature range of 350–425 °C. When Ti was introduced, all of the Ce-Zr-Ti oxide catalysts exhibited much better activities. With the increase in Ti content, the low temperature firstly increased and then decreased. As a result, the  $\text{CeZr}_{0.5}\text{Ti}_2\text{O}_x$  catalyst presented the best activity in a low temperature range, together with a high  $\text{NO}_x$  conversion in a wide temperature range. On the other hand, the variation in high temperature activity with Ti content was contrary to that of low temperature activity, with the activity of  $\text{CeZr}_{0.5}\text{Ti}_2\text{O}_x$  slightly lower than those of the other Ce-Zr-Ti oxide catalysts in a high temperature range. In addition, adding Ti to the catalyst also enhanced the  $\text{N}_2$  selectivity, and the Ce-Zr-Ti oxide catalysts all presented higher  $\text{N}_2$  selectivity than  $\text{CeZr}_{0.5}\text{O}_x$  (Figure 1B).



**Figure 1.** (A)  $\text{NO}_x$  conversions and (B)  $\text{N}_2$  selectivity over the  $\text{CeZr}_{0.5}\text{O}_x$  and Ce-Zr-Ti oxide catalysts. Reaction conditions:  $[\text{NO}] = [\text{NH}_3] = 500 \text{ ppm}$ ,  $[\text{O}_2] = 5 \text{ vol.}\%$ ,  $\text{N}_2$  balance, and  $\text{GHSV} = 200,000 \text{ h}^{-1}$ .

The influences of  $\text{H}_2\text{O}$  and space velocity on the  $\text{NO}_x$  conversion over  $\text{CeZr}_{0.5}\text{Ti}_2\text{O}_x$  were tested and the results are shown in Figure 2. The existence of 5%  $\text{H}_2\text{O}$  in the flow gas decreased the low temperature activity, but enhanced the high temperature activity. As a result, over 80%  $\text{NO}_x$  conversion could still be achieved from 250 to 450 °C. When the GHSV was decreased from 200,000  $\text{h}^{-1}$  to 100,000  $\text{h}^{-1}$ , the activity of the catalyst at low temperatures was obviously improved.



**Figure 2.**  $\text{NO}_x$  conversion over  $\text{CeZr}_{0.5}\text{Ti}_2\text{O}_x$  catalyst under different reaction conditions. Reaction conditions:  $[\text{NO}] = [\text{NH}_3] = 500$  ppm,  $[\text{O}_2] = 5$  vol.%,  $[\text{H}_2\text{O}] = 5$  vol.% (when used),  $\text{N}_2$  balance, and GHSV = 100,000 or 200,000  $\text{h}^{-1}$ .

## 2.2. Separated $\text{NO}/\text{NH}_3$ Oxidation

To analyze the effects of Ti on the catalyst, separated  $\text{NO}$  oxidation and  $\text{NH}_3$  oxidation tests were carried out for the  $\text{CeZr}_{0.5}\text{O}_x$  and  $\text{CeZr}_{0.5}\text{Ti}_2\text{O}_x$  (Figure 3). The  $\text{NO}_2$  production during  $\text{NO}$  oxidation over the  $\text{CeZr}_{0.5}\text{Ti}_2\text{O}_x$  was clearly higher than that over  $\text{CeZr}_{0.5}\text{O}_x$  at a low temperature. Since the presentation of  $\text{NO}_2$  in the reaction gas could promote the SCR reaction at a low temperature by accelerating the fast SCR process ( $2\text{NH}_3 + \text{NO} + \text{NO}_2 \rightarrow 2\text{N}_2 + 3\text{H}_2\text{O}$ ), the enhanced low-temperature activity by the introduction of Ti should be associated with the promoted oxidation of  $\text{NO}$  to  $\text{NO}_2$  over  $\text{CeZr}_{0.5}\text{Ti}_2\text{O}_x$  [10,35]. In addition, the introduction of Ti also promoted  $\text{NH}_3$  oxidation over the catalyst at a high temperature. The  $\text{NH}_3$ -SCR reaction route at a high temperature mainly follows the Eley-Rideal mechanism, and the activation of  $\text{NH}_3$  to form  $\text{NH}_2$  species by oxidation plays the key role for the reaction with  $\text{NO}$  to form  $\text{N}_2$  and  $\text{H}_2\text{O}$ , owing to  $\text{NH}_2 + \text{NO}(\text{g}) \rightarrow \text{N}_2 + \text{H}_2\text{O}$ . Therefore, promoted  $\text{NH}_3$  oxidation would be beneficial for the improvement of high temperature activity.

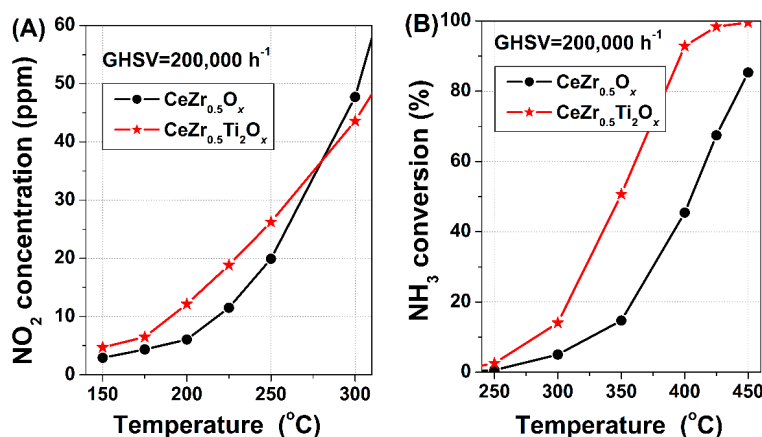


**Figure 3.** (A)  $\text{NO}_2$  productions during separate  $\text{NO}$  oxidation reaction and (B)  $\text{NH}_3$  conversions during separate  $\text{NH}_3$  oxidation reaction over the  $\text{CeZr}_{0.5}\text{O}_x$  and  $\text{CeZr}_{0.5}\text{Ti}_2\text{O}_x$  catalysts. Reaction conditions: (A)  $[\text{NO}]_{\text{ENREF}_30} = 500$  ppm, (B)  $[\text{NH}_3] = 500$  ppm,  $[\text{O}_2] = 5$  vol.%,  $\text{N}_2$  balance and GHSV = 200,000  $\text{h}^{-1}$ .

### 2.3. XRD

The X-ray diffraction (XRD) results of the  $\text{CeZr}_{0.5}\text{O}_x$  and Ce-Z-Ti oxide catalysts are presented in Figure 4. Both  $\text{CeO}_2$  and  $\text{ZrO}_2$  were detected in  $\text{CeZr}_{0.5}\text{O}_x$ . With the increase of Ti, the peaks for  $\text{CeO}_2$  and  $\text{ZrO}_2$  became more and more weak, and only anatase  $\text{TiO}_2$  was observed for  $\text{CeZr}_{0.5}\text{Ti}_{10}\text{O}_x$ . Only weak peaks for  $\text{CeO}_2$  with cubic fluorite structures (PDF# 43-1002) were observed in the  $\text{CeZr}_{0.5}\text{Ti}_2\text{O}_x$ , indicating that the introduction of Ti had induced the structural change of the  $\text{CeZr}_{0.5}\text{O}_x$ , and the crystallizations of Ce, Zr and Ti oxides in  $\text{CeZr}_{0.5}\text{Ti}_2\text{O}_x$  were significantly inhibited. As a result, the  $\text{CeZr}_{0.5}\text{Ti}_2\text{O}_x$  ( $165.1 \text{ m}^2/\text{g}$ ) showed a higher Brunauer–Emmett–Teller (BET) surface area than  $\text{CeZr}_{0.5}\text{O}_x$  ( $113.5 \text{ m}^2/\text{g}$ ).

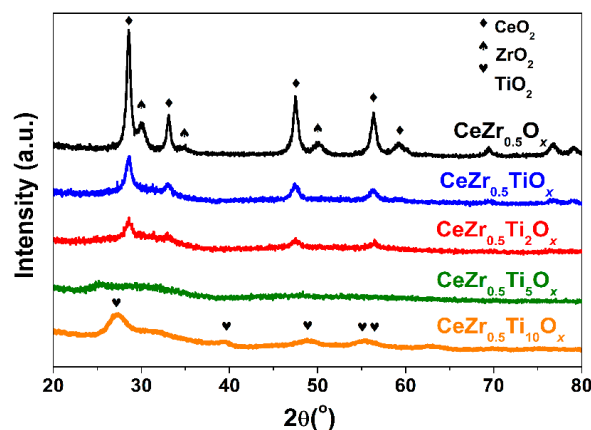


Figure 4. XRD patterns of the  $\text{CeZr}_{0.5}\text{O}_x$  and Ce-Z-Ti oxide catalysts.

### 2.4. $\text{H}_2$ -TPR

The  $\text{H}_2$  temperature-programmed reduction ( $\text{H}_2$ -TPR) profiles of  $\text{CeZr}_{0.5}\text{O}_x$  and  $\text{CeZr}_{0.5}\text{Ti}_2\text{O}_x$  are presented in Figure 5. The  $\text{CeZr}_{0.5}\text{O}_x$  exhibited two peaks at 496 and 755 °C due to the surface and bulk reductions of  $\text{CeO}_2$  (as detected by XRD), respectively [31,36–38]. During the test, coordinatively unsaturated surface oxygen anions are easily reduced by  $\text{H}_2$  in the low temperature region, while the bulk oxygen species are reduced only after the transportation to the surface [39]. With the addition of Ti, a sharp  $\text{H}_2$  consumption peak appeared at 567 °C, which indicates that another type of Ce species might be formed. Considering the XRD results, this sharp peak might be associated with the reduction of the highly dispersed Ce species from  $\text{Ce}^{4+}$  to  $\text{Ce}^{3+}$  [22,34]. In addition, the  $\text{H}_2$  consumption of  $\text{CeZr}_{0.5}\text{Ti}_2\text{O}_x$  was much higher than that of  $\text{CeZr}_{0.5}\text{O}_x$  at a low temperature. The  $\text{H}_2$ -TPR results clearly indicated the enhancement of redox functions for  $\text{CeZr}_{0.5}\text{Ti}_2\text{O}_x$ .

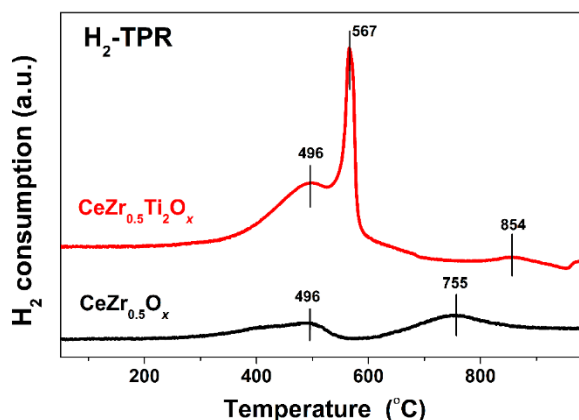
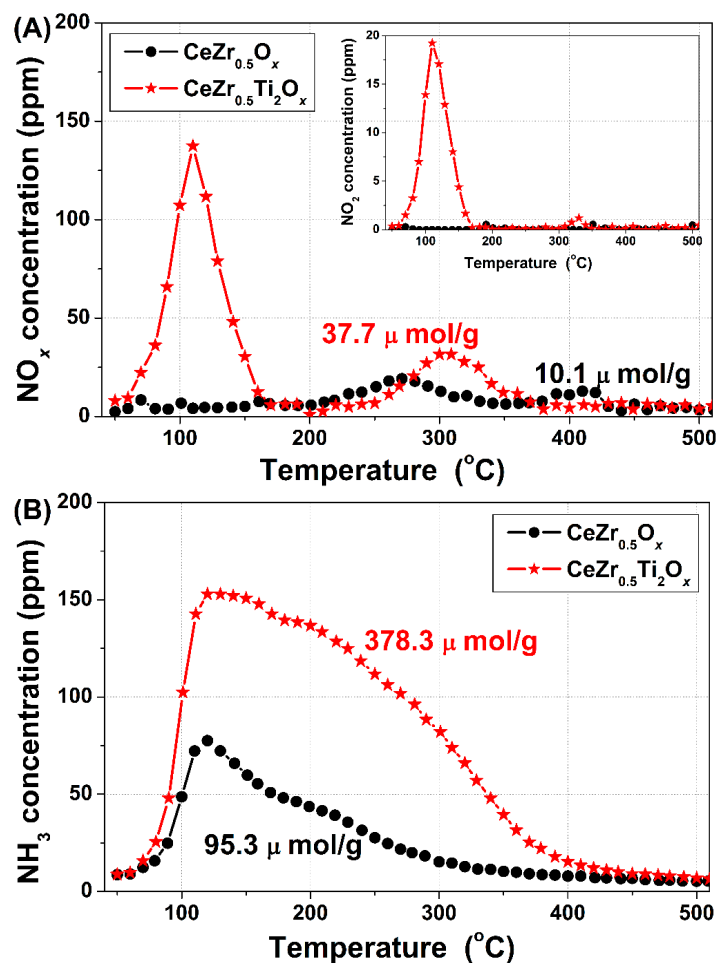


Figure 5.  $\text{H}_2$ -TPR profiles of the  $\text{CeZr}_{0.5}\text{O}_x$  and  $\text{CeZr}_{0.5}\text{Ti}_2\text{O}_x$  catalysts.

Previous studies have indicated that the redox properties of  $\text{NH}_3$ -SCR catalyst play a dominant role in the low temperature activity [35,40,41]. Therefore, the enhanced redox function of  $\text{CeZr}_{0.5}\text{Ti}_2\text{O}_x$  would be beneficial for low temperature activity.

## 2.5. $\text{NO}_x/\text{NH}_3$ -TPD

To investigate the  $\text{NO}_x$  and  $\text{NH}_3$  adsorption/desorption properties of  $\text{CeZr}_{0.5}\text{O}_x$  and  $\text{CeZr}_{0.5}\text{Ti}_2\text{O}_x$ ,  $\text{NO}_x$  temperature-programmed desorption ( $\text{NO}_x$ -TPD) and  $\text{NH}_3$  temperature-programmed desorption ( $\text{NH}_3$ -TPD) were performed for the catalysts (Figure 6).



**Figure 6.** (A)  $\text{NO}_x$ -TPD and (B)  $\text{NH}_3$ -TPD profiles of the  $\text{CeZr}_{0.5}\text{O}_x$  and  $\text{CeZr}_{0.5}\text{Ti}_2\text{O}_x$  catalysts.

The  $\text{NO}_x$ -TPD profiles are presented in Figure 6A. The first  $\text{NO}_x$  peak of  $\text{CeZr}_{0.5}\text{Ti}_2\text{O}_x$  was at ca. 110  $^{\circ}\text{C}$ , mainly due to the desorption of physisorbed  $\text{NO}_x$ , while the other  $\text{NO}_x$  peak was at ca. 300  $^{\circ}\text{C}$  and was associated with the decomposition of chemisorbed  $\text{NO}_x$  species [42,43]. On the other hand, two weak peaks were observed for  $\text{CeZr}_{0.5}\text{O}_x$  at ca. 270  $^{\circ}\text{C}$  and ca. 410  $^{\circ}\text{C}$ , respectively, which were due to the decomposition of different types of chemisorbed  $\text{NO}_x$  species. With the addition of Ti, the adsorbed  $\text{NO}_x$  on  $\text{CeZr}_{0.5}\text{Ti}_2\text{O}_x$  was obviously more than that of  $\text{CeZr}_{0.5}\text{O}_x$ . Particularly, the desorbed  $\text{NO}_2$  of  $\text{CeZr}_{0.5}\text{Ti}_2\text{O}_x$  was much higher, owing to the enhanced low-temperature activity for NO oxidation (as shown by the separated NO oxidation results), which could facilitate the conversion of  $\text{NO}_x$  in  $\text{NH}_3$ -SCR.

Surface acidity plays a dominate role in the high-temperature SCR activity due to its effects on the adsorption and activation of  $\text{NH}_3$  [35,41]. Previous studies have revealed that Ti species of  $\text{NH}_3$ -SCR catalysts mainly act as acid sites in the reaction for  $\text{NH}_3$  adsorption [4]. Therefore, the adsorbed  $\text{NH}_3$

of  $\text{CeZr}_{0.5}\text{Ti}_2\text{O}_x$  was much more than that of  $\text{CeZr}_{0.5}\text{O}_x$ , which might be an important reason for the better  $\text{NH}_3$ -SCR activity of  $\text{CeZr}_{0.5}\text{Ti}_2\text{O}_x$  at high temperatures.

## 2.6. XPS

The X-ray photoelectron spectroscopy (XPS) results for Ce 3d of the  $\text{CeZr}_{0.5}\text{O}_x$  and  $\text{CeZr}_{0.5}\text{Ti}_2\text{O}_x$  are shown in Figure 7. The sub-bands labeled with  $u'/v'$  and  $u^0/v^0$  represent the  $3d^{10}4f^1$  initial electronic state corresponding to  $\text{Ce}^{3+}$  and the  $3d^94f^2$  state of  $\text{Ce}^{3+}$ , respectively [44]. The sub-bands labeled with  $u'''$  and  $v'''$  represent the  $3d^{10}4f^0$  state of  $\text{Ce}^{4+}$ , and the sub-bands labeled with  $u$ ,  $u''$ ,  $v$  and  $v''$  represent the  $3d^94f^1$  state corresponding to  $\text{Ce}^{4+}$  [44]. The presence of  $\text{Ce}^{3+}$  would induce a charge imbalance, which could lead to unsaturated chemical bonds and oxygen vacancies. The calculated  $\text{Ce}^{3+}$  ratio of  $\text{CeZr}_{0.5}\text{Ti}_2\text{O}_x$  (36.0%) was higher than that of  $\text{CeZr}_{0.5}\text{O}_x$  (33.8%), indicating that more surface oxygen vacancies presented in  $\text{CeZr}_{0.5}\text{Ti}_2\text{O}_x$ . In addition, the  $\text{Ce}^{3+}$  ratio of the catalyst could influence the redox ability and reactant adsorption and activation functions, and thereby contribute to  $\text{NH}_3$ -SCR performance.

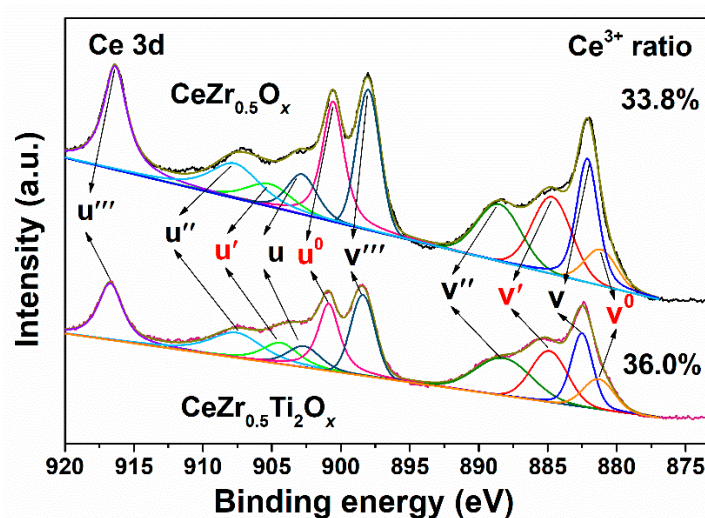


Figure 7. XPS results of Ce 3d of the  $\text{CeZr}_{0.5}\text{O}_x$  and  $\text{CeZr}_{0.5}\text{Ti}_2\text{O}_x$  catalysts.

The surface oxygen vacancies of the catalysts might generate weakly-adsorbed oxygen species or additional chemisorbed oxygen on the surface of the catalyst [27,45]. The XPS results of O 1s of the  $\text{CeZr}_{0.5}\text{O}_x$  and  $\text{CeZr}_{0.5}\text{Ti}_2\text{O}_x$  are shown in Figure 8. The O 1s peak was fit into two sub-bands. The sub-bands at 531.2–531.5 eV and 529.1–529.6 eV were assigned to the surface adsorbed oxygen ( $\text{O}_\alpha$ ), such as the  $\text{O}_2^{2-}$  and  $\text{O}^-$  belonging to defect-oxide or a hydroxyl-like group, and the lattice oxygen  $\text{O}^{2-}$  ( $\text{O}_\beta$ ), respectively [46]. The  $\text{O}_\alpha$  ratios of the catalysts were calculated by  $\text{O}_\alpha/(\text{O}_\alpha + \text{O}_\beta)$ , and the  $\text{CeZr}_{0.5}\text{Ti}_2\text{O}_x$  showed higher  $\text{O}_\alpha$  ratio than  $\text{CeZr}_{0.5}\text{O}_x$ . The results confirmed that the addition of Ti indeed induced more surface-adsorbed oxygen, which would facilitate NO oxidation to  $\text{NO}_2$  (as shown by the separated NO oxidation and  $\text{NO}_x$ -TPD results), and thus facilitates the conversion of NO by fast SCR effects.

## 2.7. Formation Process Analysis of the $\text{CeZr}_{0.5}\text{Ti}_2\text{O}_x$ Catalyst

Figure 9 shows the pH variations of the mixed solutions for the preparation of the  $\text{CeZr}_{0.5}\text{O}_x$  and  $\text{CeZr}_{0.5}\text{Ti}_2\text{O}_x$  catalysts. During the preparation of  $\text{CeZr}_{0.5}\text{O}_x$ , the initial pH value of the solution was 1.6. With the hydrolysis of urea, the pH increased gradually to be 7.6 after heating for 12 h. Due to the increase in pH, suspended particles began to appear in the solution in the second hour. The particles with the precipitation time of 2 h, 4 h, 6 h, and 12 h were collected and then calcined to be catalyst samples. The activity tests of these samples showed similar  $\text{NO}_x$  conversions with each other.



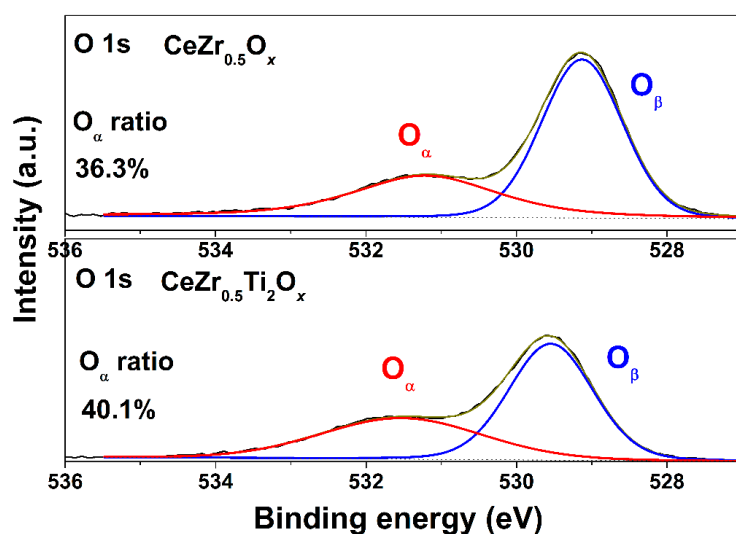


Figure 8. XPS results of O 1s of the  $\text{CeZr}_{0.5}\text{O}_x$  and  $\text{CeZr}_{0.5}\text{Ti}_2\text{O}_x$  catalysts.

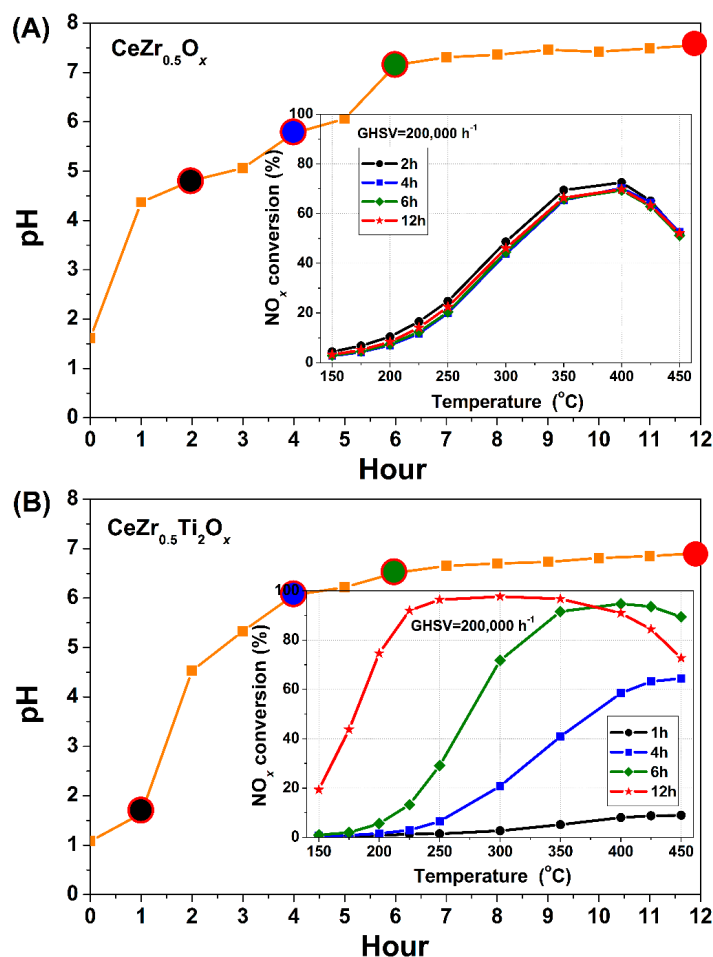
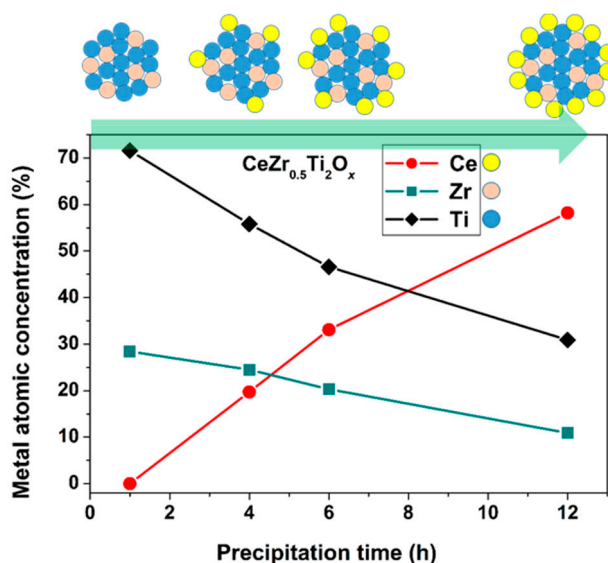


Figure 9. The pH variation of the mixed solution during the preparation of the (A)  $\text{CeZr}_{0.5}\text{O}_x$  and (B)  $\text{CeZr}_{0.5}\text{Ti}_2\text{O}_x$  catalysts, and the  $\text{NO}_x$  conversions of the obtained samples at different precipitation time.

Due to the acidity induced by the added  $\text{Ti}(\text{SO}_4)_2$ , the initial pH value of the mixed solution during the preparation of  $\text{CeZr}_{0.5}\text{Ti}_2\text{O}_x$  dropped to be 1.1. With the hydrolysis of urea, the pH increased gradually after heating, and some white particles generated in the first hour and suspended in the

solution. With the increase of time, the particles gradually turned yellow. The pH reached ca. 7.0 after 12 h of reaction. The particles with the precipitation times of 1 h, 4 h, 6 h, and 12 h were collected and then calcined to be catalyst samples. Interestingly, the activity test showed a remarkable enhancement of  $\text{NO}_x$  conversions for the four samples with the increase in precipitation time.

The surface metal atomic concentrations of the  $\text{CeZr}_{0.5}\text{Ti}_2\text{O}_x$  samples with different precipitation times were analyzed using XPS, and the variations in Ce, Zr, and Ti concentrations with precipitation time are shown in Figure 10. For the 1-h precipitation sample, only Ti and Zr, without Ce, were detected. With the increase in precipitation time, surface Ce concentration increased gradually in the samples. At the same time, Ti and Zr concentrations gradually decreased with the increase in precipitation time. A TEM-EDS mapping image showed that Ce was highly dispersed in the  $\text{CeZr}_{0.5}\text{Ti}_2\text{O}_x$  catalyst (Figure 11).



**Figure 10.** Surface metal atomic concentrations of the  $\text{CeZr}_{0.5}\text{Ti}_2\text{O}_x$  samples with different precipitation times.

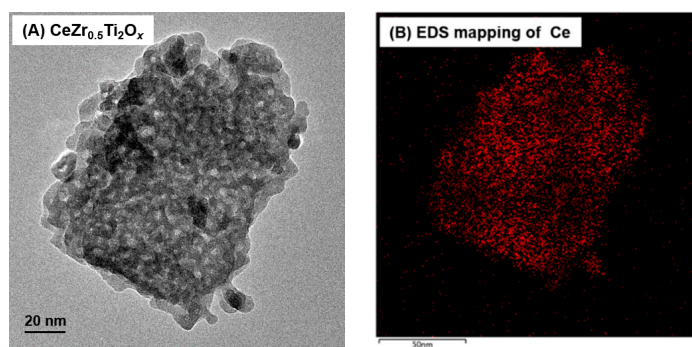


**Figure 11.** TEM image (A) and the corresponding EDS mapping (B) for the Ce of the  $\text{CeZr}_{0.5}\text{Ti}_2\text{O}_x$  catalyst.

Considering the variations in the solution pH value when preparing the  $\text{CeZr}_{0.5}\text{Ti}_2\text{O}_x$ , the formation process of the catalyst can be proposed as follows: The Ti and Zr species were first co-precipitated with the increase in solution pH. Then, the Ce species uniformly precipitated onto the precipitated Zr-Ti species with the further increase in pH. Finally, a  $\text{CeZr}_{0.5}\text{Ti}_2\text{O}_x$  catalyst with a higher surface Ce concentration than Ti and Zr was obtained. Through control of the hydrolysis of urea, the variations in the solution pH can be controlled, and then we can control the precipitation process of



the catalyst, which is very important for the formation of highly-dispersed CeO<sub>2</sub> on ZrO<sub>2</sub>-TiO<sub>2</sub>. Thus, the obtained catalyst can present excellent NH<sub>3</sub>-SCR performance.

### 3. Experimental Section

#### 3.1. Catalyst Preparation and Activity Test

The CeZr<sub>0.5</sub>Ti<sub>a</sub>O<sub>x</sub> (a = Ti/Ce molar ratio = 0, 1, 2, 5, 10), with a Zr/Ce molar ratio fixed to be 0.5, was prepared using a precipitation method. Desired precursors of Ce(NO<sub>3</sub>)<sub>3</sub>·6H<sub>2</sub>O (>99%, Sinopharm Chemical Reagent Co., Ltd., Shanghai, China), Zr(NO<sub>3</sub>)<sub>4</sub>·5H<sub>2</sub>O (>99%, Sinopharm Chemical Reagent Co., Ltd., Shanghai, China) and Ti(SO<sub>4</sub>)<sub>2</sub> (>98%, Sinopharm Chemical Reagent Co., Ltd., Shanghai, China) were dissolved together in distilled water, and urea (>99%, Sinopharm Chemical Reagent Co., Ltd., Shanghai, China) was added to the mixed solution as a slowly-releasing precipitator. Then, the solution was heated to 90 °C to facilitate the release of NH<sub>3</sub> and thereby raise the pH value gradually. The temperature of the mixed solution was held at 90 °C for 12 h under vigorous stirring (some samples with shorter precipitation times were also prepared). After that, the precipitated powders were collected via filtration, washed using distilled water, and dried for 12 h at 100 °C. Finally, the catalyst was obtained after calcination at 500 °C for 5 h.

The SCR activity of the catalysts (40–60 mesh) were tested in a fixed-bed quartz flow reactor. The reaction conditions were controlled as follows: 500 ppm NO, 500 ppm NH<sub>3</sub>, 5 vol.% O<sub>2</sub>, N<sub>2</sub> balance, and 400 mL/min total flow rate. Different gas hourly space velocities (GHSVs) were obtained by changing the volume of catalysts, i.e., 0.24 mL catalyst for a GHSV = 100,000 h<sup>−1</sup> and 0.12 mL catalyst for a GHSV = 200,000 h<sup>−1</sup>. The concentrations of effluent N-containing gases (NO, NH<sub>3</sub>, NO<sub>2</sub> and N<sub>2</sub>O) were continuously measured by an online FTIR gas analyzer (Nicolet Antaris IGS analyzer, Thermo-Fisher Scientific, Waltham, MA, USA). NO<sub>x</sub> conversion and N<sub>2</sub> selectivity were calculated using the following equations, respectively:

$$\text{NO}_x \text{ conversion} = \left(1 - \frac{[\text{NO}]_{\text{out}} + [\text{NO}_2]_{\text{out}}}{[\text{NO}]_{\text{in}} + [\text{NO}_2]_{\text{in}}}\right) \times 100\%$$

$$\text{N}_2 \text{ selectivity} = \left(1 - \frac{2[\text{N}_2\text{O}]_{\text{out}}}{[\text{NO}_x]_{\text{in}} + [\text{NH}_3]_{\text{in}} - [\text{NO}_x]_{\text{out}} - [\text{NH}_3]_{\text{out}}}\right) \times 100\%$$

#### 3.2. Characterizations

X-ray diffraction (XRD) measurements were carried out on a computerized AXS D8 diffractometer (Bruker, GER), with Cu Kα (λ = 0.15406 nm) radiation, from 20 to 80° at 8°/min.

Surface areas were tested using an ASAP 2020 (Micromeritics, Norcross, GA, USA) at −196 °C by N<sub>2</sub> adsorption/desorption and calculated using a BET equation in the 0.05–0.35 partial pressure range.

The X-ray photoelectron spectroscopy (XPS) results of Ce 3d and O 1s were measured on an ESCALAB 250Xi Scanning X-ray Microprobe (Thermo-Fisher Scientific, Waltham, MA, USA) using Al Kα radiation (1486.7 eV) and a C 1 s peak, with BE = 284.8 eV as the calibration standard.

The transmission electron microscopy (TEM) image and energy-dispersive X-ray spectroscopy (EDS) mapping of Ce were obtained using a JEM-2100F equipment (JEOL, Tokyo, Japan), combined with a specimen tilting beryllium holder for energy dispersive spectroscopy. The accelerating voltage was 200 kV.

The H<sub>2</sub> temperature-programmed reduction (H<sub>2</sub>-TPR) was tested using an AutoChem\_II\_2920 chemisorption analyzer (Micromeritics, Norcross, GA, USA), and the temperature-programmed desorption of NH<sub>3</sub> and NO<sub>x</sub> (NO<sub>x</sub>-TPD and NH<sub>3</sub>-TPD) were tested using the same reaction system as the activity tests. Experiment details can be found in Reference [42].

#### 4. Conclusions

A series of Ce-Zr-Ti oxide catalysts were prepared using a stepwise precipitation approach for  $\text{NH}_3$ -SCR.  $\text{CeZr}_{0.5}\text{O}_x$  without Ti just showed a relatively low  $\text{NO}_x$  conversion. When Ti was introduced, Ce-Zr-Ti catalysts showed much better activities and  $\text{N}_2$  selectivity. A  $\text{CeZr}_{0.5}\text{Ti}_2\text{O}_x$  catalyst, which contains moderate Ti amounts, showed the best performance, which is associated with its optimal ratios for the redox ( $\text{CeO}_x$ ) and acidic ( $\text{TiO}_2$ ) components.

$\text{CeZr}_{0.5}\text{O}_x$  and  $\text{CeZr}_{0.5}\text{Ti}_2\text{O}_x$  catalysts were characterized using various methods and the formation process during preparation was investigated.  $\text{CeZr}_{0.5}\text{Ti}_2\text{O}_x$  catalyst showed superior redox properties (by  $\text{H}_2$ -TPR), good adsorption and  $\text{NO}_x/\text{NH}_3$  activation functions (by  $\text{NO}_x$ -TPD and  $\text{NH}_3$ -TPD, respectively), and enhanced charge imbalance (by XPS).

During preparation, the Ti and Zr species were first co-precipitated with an increase in solution pH. Then, the Ce species uniformly precipitated onto the precipitated Zr-Ti species with the further increase in pH. As a result,  $\text{CeZr}_{0.5}\text{Ti}_2\text{O}_x$  catalyst with a surface Ce concentration higher than those of Ti and Zr was obtained. This preparation process resulted in the formation of highly-dispersed  $\text{CeO}_2$  on  $\text{ZrO}_2\text{-TiO}_2$ , and thus the catalyst can present excellent  $\text{NH}_3$ -SCR performance.

**Author Contributions:** W.S. and H.H. conceived the project; Y.G. and Y.Z. performed the experiments; W.S. and Z.L. carried out the data analysis; W.S. and Y.G. wrote the paper; H.H. supervised the study.

**Funding:** This work was supported by the National Key R&D Program of China (2017YFC0212502, 2017YFC0211101), the National Natural Science Foundation of China (201637005), and the Key Research Program of the Chinese Academy of Sciences (ZDRW-ZS-2017-6-2-3).

**Conflicts of Interest:** The authors declare no conflicts of interest.

#### References

1. Parvulescu, V.I.; Granger, P.; Delmon, B. Catalytic removal of  $\text{NO}$ . *Catal. Today* **1998**, *46*, 233–316. [[CrossRef](#)]
2. Granger, P.; Parvulescu, V.I. Catalytic  $\text{NO}_x$  abatement systems for mobile sources: From three-way to lean burn after-treatment technologies. *Chem. Rev.* **2011**, *111*, 3155–3207. [[CrossRef](#)] [[PubMed](#)]
3. Liu, Z.; Woo, S.I. Recent advances in catalytic  $\text{DeNO}_x$  science and technology. *Catal. Rev.* **2006**, *48*, 43–89. [[CrossRef](#)]
4. Busca, G.; Lietti, L.; Ramis, G.; Berti, F. Chemical and mechanistic aspects of the selective catalytic reduction of  $\text{NO}_x$  by ammonia over oxide catalysts: A review. *Appl. Catal. B* **1998**, *18*, 1–36. [[CrossRef](#)]
5. Liu, F.; Yu, Y.; He, H. Environmentally-benign catalysts for the selective catalytic reduction of  $\text{NO}_x$  from diesel engines: Structure-activity relationship and reaction mechanism aspects. *Chem. Commun.* **2014**, *50*, 8445–8463. [[CrossRef](#)] [[PubMed](#)]
6. Shan, W.; Song, H. Catalysts for the selective catalytic reduction of  $\text{NO}_x$  with  $\text{NH}_3$  at low temperature. *Catal. Sci. Technol.* **2015**, *5*, 4280–4288. [[CrossRef](#)]
7. Guan, B.; Zhan, R.; Lin, H.; Huang, Z. Review of state of the art technologies of selective catalytic reduction of  $\text{NO}_x$  from diesel engine exhaust. *Appl. Therm. Eng.* **2014**, *66*, 395–414. [[CrossRef](#)]
8. Gao, F.; Kwak, J.; Szanyi, J.; Peden, C.F. Current understanding of Cu-exchanged chabazite molecular sieves for use as commercial diesel engine  $\text{DeNO}_x$  catalysts. *Top. Catal.* **2013**, *56*, 1441–1459. [[CrossRef](#)]
9. Brandenberger, S.; Kröcher, O.; Tissler, A.; Althoff, R. The state of the art in selective catalytic reduction of  $\text{NO}_x$  by ammonia using metal-exchanged zeolite catalysts. *Catal. Rev.* **2008**, *50*, 492–531. [[CrossRef](#)]
10. Li, J.; Chang, H.; Ma, L.; Hao, J.; Yang, R.T. Low-temperature selective catalytic reduction of  $\text{NO}_x$  with  $\text{NH}_3$  over metal oxide and zeolite catalysts—a review. *Catal. Today* **2011**, *175*, 147–156. [[CrossRef](#)]
11. Deka, U.; Lezcano-Gonzalez, I.; Weckhuysen, B.M.; Beale, A.M. Local environment and nature of Cu active sites in zeolite-based catalysts for the selective catalytic reduction of  $\text{NO}_x$ . *ACS Catal.* **2013**, *4*, 413–427. [[CrossRef](#)]
12. Li, Y.; Cheng, H.; Li, D.; Qin, Y.; Xie, Y.; Wang, S.  $\text{WO}_3/\text{CeO}_2\text{-ZrO}_2$ , a promising catalyst for selective catalytic reduction (SCR) of  $\text{NO}_x$  with  $\text{NH}_3$  in diesel exhaust. *Chem. Commun.* **2008**, 1470–1472. [[CrossRef](#)] [[PubMed](#)]

13. Can, F.; Berland, S.; Royer, S.; Courtois, X.; Duprez, D. Composition-dependent performance of  $\text{Ce}_x\text{Zr}_{1-x}\text{O}_2$  mixed-oxide-supported  $\text{WO}_3$  catalysts for the  $\text{NO}_x$  storage reduction–selective catalytic reduction coupled process. *ACS Catal.* **2013**, *3*, 1120–1132. [[CrossRef](#)]
14. Long, R.Q.; Yang, R.T. Superior Fe-ZSM-5 catalyst for selective catalytic reduction of nitric oxide by ammonia. *J. Am. Chem. Soc.* **1999**, *121*, 5595–5596. [[CrossRef](#)]
15. Chen, L.; Li, J.; Ge, M. Promotional effect of Ce-doped  $\text{V}_2\text{O}_5\text{-WO}_3/\text{TiO}_2$  with low vanadium loadings for selective catalytic reduction of  $\text{NO}_x$  by  $\text{NH}_3$ . *J. Phys. Chem. C* **2009**, *113*, 21177–21184. [[CrossRef](#)]
16. Wu, Z.; Jin, R.; Liu, Y.; Wang, H. Ceria modified  $\text{MnO}_x/\text{TiO}_2$  as a superior catalyst for NO reduction with  $\text{NH}_3$  at low-temperature. *Catal. Commun.* **2008**, *9*, 2217–2220. [[CrossRef](#)]
17. Niu, C.; Shi, X.; Liu, K.; You, Y.; Wang, S.; He, H. A novel one-pot synthesized CuCe-SAPO-34 catalyst with high  $\text{NH}_3$ -SCR activity and  $\text{H}_2\text{O}$  resistance. *Catal. Commun.* **2016**, *81*, 20–23. [[CrossRef](#)]
18. Carja, G.; Delahay, G.; Signorile, C.; Coq, B. Fe-Ce-ZSM-5 a new catalyst of outstanding properties in the selective catalytic reduction of NO with  $\text{NH}_3$ . *Chem. Commun.* **2004**, 1404–1405. [[CrossRef](#)] [[PubMed](#)]
19. Gao, X.; Jiang, Y.; Fu, Y.; Zhong, Y.; Luo, Z.; Cen, K. Preparation and characterization of  $\text{CeO}_2/\text{TiO}_2$  catalysts for selective catalytic reduction of NO with  $\text{NH}_3$ . *Catal. Commun.* **2010**, *11*, 465–469. [[CrossRef](#)]
20. Liu, Z.; Yi, Y.; Li, J.; Woo, S.I.; Wang, B.; Cao, X.; Li, Z. A superior catalyst with dual redox cycles for the selective reduction of  $\text{NO}_x$  by ammonia. *Chem. Commun.* **2013**, 49, 7726–7728. [[CrossRef](#)] [[PubMed](#)]
21. Liu, Z.; Zhang, S.; Li, J.; Ma, L. Promoting effect of  $\text{MoO}_3$  on the  $\text{NO}_x$  reduction by  $\text{NH}_3$  over  $\text{CeO}_2/\text{TiO}_2$  catalyst studied with in situ DRIFTS. *Appl. Catal. B* **2014**, *144*, 90–95. [[CrossRef](#)]
22. Peng, Y.; Qu, R.; Zhang, X.; Li, J. The relationship between structure and activity of  $\text{MoO}_3\text{-CeO}_2$  catalysts for NO removal: Influences of acidity and reducibility. *Chem. Commun.* **2013**, 49, 6215–6217. [[CrossRef](#)] [[PubMed](#)]
23. Qu, R.; Gao, X.; Cen, K.; Li, J. Relationship between structure and performance of a novel cerium-niobium binary oxide catalyst for selective catalytic reduction of NO with  $\text{NH}_3$ . *Appl. Catal. B* **2013**, *142*, 290–297. [[CrossRef](#)]
24. Shan, W.; Liu, F.; He, H.; Shi, X.; Zhang, C. Novel cerium-tungsten mixed oxide catalyst for the selective catalytic reduction of  $\text{NO}_x$  with  $\text{NH}_3$ . *Chem. Commun.* **2011**, 47, 8046–8048. [[CrossRef](#)] [[PubMed](#)]
25. Krishna, K.; Seijger, G.B.F.; Bleek, C.M.; Calis, H.P.A. Very active  $\text{CeO}_2$ -zeolite catalysts for  $\text{NO}_x$  reduction with  $\text{NH}_3$ . *Chem. Commun.* **2002**, 18, 2030–2031. [[CrossRef](#)]
26. Shan, W.; Liu, F.; Yu, Y.; He, H. The use of ceria for the selective catalytic reduction of  $\text{NO}_x$  with  $\text{NH}_3$ . *Chin. J. Catal.* **2014**, *35*, 1251–1259. [[CrossRef](#)]
27. Gu, T.; Liu, Y.; Weng, X.; Wang, H.; Wu, Z. The enhanced performance of ceria with surface sulfation for selective catalytic reduction of NO by  $\text{NH}_3$ . *Catal. Commun.* **2010**, *12*, 310–313. [[CrossRef](#)]
28. Zhang, L.; Pierce, J.; Leung, V.L.; Wang, D.; Epling, W.S. Characterization of ceria's interaction with  $\text{NO}_x$  and  $\text{NH}_3$ . *J. Phys. Chem. C* **2013**, *117*, 8282–8289. [[CrossRef](#)]
29. Si, Z.; Weng, D.; Wu, X.; Yang, J.; Wang, B. Modifications of  $\text{CeO}_2\text{-ZrO}_2$  solid solutions by nickel and sulfate as catalysts for NO reduction with ammonia in excess  $\text{O}_2$ . *Catal. Commun.* **2010**, *11*, 1045–1048. [[CrossRef](#)]
30. Si, Z.; Weng, D.; Wu, X.; Ran, R.; Ma, Z.  $\text{NH}_3$ -SCR activity, hydrothermal stability, sulfur resistance and regeneration of  $\text{Ce}_{0.75}\text{Zr}_{0.25}\text{O}_2\text{-PO}_4^{3-}$  catalyst. *Catal. Commun.* **2012**, *17*, 146–149. [[CrossRef](#)]
31. Shen, B.; Wang, Y.; Wang, F.; Liu, T. The effect of Ce-Zr on  $\text{NH}_3$ -SCR activity over  $\text{MnO}_x(0.6)/\text{Ce}_{0.5}\text{Zr}_{0.5}\text{O}_2$  at low temperature. *Chem. Eng. J.* **2014**, *236*, 171–180. [[CrossRef](#)]
32. Ko, J.H.; Park, S.H.; Jeon, J.-K.; Kim, S.-S.; Kim, S.C.; Kim, J.M.; Chang, D.; Park, Y.-K. Low temperature selective catalytic reduction of NO with  $\text{NH}_3$  over Mn supported on  $\text{Ce}_{0.65}\text{Zr}_{0.35}\text{O}_2$  prepared by supercritical method: Effect of Mn precursors on NO reduction. *Catal. Today* **2012**, *185*, 290–295. [[CrossRef](#)]
33. Liu, Z.; Su, H.; Li, J.; Li, Y. Novel  $\text{MoO}_3/\text{CeO}_2\text{-ZrO}_2$  catalyst for the selective catalytic reduction of  $\text{NO}_x$  by  $\text{NH}_3$ . *Catal. Commun.* **2015**, *65*, 51–54. [[CrossRef](#)]
34. Ding, S.P.; Liu, F.D.; Shi, X.Y.; Liu, K.; Lian, Z.H.; Xie, L.J.; He, H. Significant promotion effect of Mo additive on a novel Ce-Zr mixed oxide catalyst for the selective catalytic reduction of  $\text{NO}_x$  with  $\text{NH}_3$ . *ACS Appl. Mater. Interfaces* **2015**, *7*, 9497–9506. [[CrossRef](#)] [[PubMed](#)]
35. Shan, W.; Liu, F.; He, H.; Shi, X.; Zhang, C. A superior Ce-W-Ti mixed oxide catalyst for the selective catalytic reduction of  $\text{NO}_x$  with  $\text{NH}_3$ . *Appl. Catal. B* **2012**, *115–116*, 100–106. [[CrossRef](#)]
36. Chen, A.; Zhou, Y.; Ta, N.; Li, Y.; Shen, W. Redox properties and catalytic performance of ceria-zirconia nanorods. *Catal. Sci. Technol.* **2015**, *5*, 4184–4192. [[CrossRef](#)]

37. Liu, Z.; Zhang, S.; Li, J.; Zhu, J.; Ma, L. Novel  $V_2O_5$ - $CeO_2$ / $TiO_2$  catalyst with low vanadium loading for the selective catalytic reduction of  $NO_x$  by  $NH_3$ . *Appl. Catal. B* **2014**, *158–159*, 11–19. [[CrossRef](#)]
38. Vuong, T.H.; Radnik, J.; Rabeah, J.; Bentrup, U.; Schneider, M.; Atia, H.; Armbruster, U.; Grünert, W.; Brückner, A. Efficient  $VO_x/Ce_{1-x}Ti_xO_2$  catalysts for low-temperature  $NH_3$ -SCR: Reaction mechanism and active sites assessed by in situ/operando spectroscopy. *ACS Catal.* **2017**, *7*, 1693–1705. [[CrossRef](#)]
39. Wang, Z.; Qu, Z.; Quan, X.; Wang, H. Selective catalytic oxidation of ammonia to nitrogen over ceria–zirconia mixed oxides. *Appl. Catal. A* **2012**, *411–412*, 131–138. [[CrossRef](#)]
40. Topsøe, N.-Y. Mechanism of the selective catalytic reduction of nitric oxide by ammonia elucidated by in situ on-line Fourier Transform Infrared Spectroscopy. *Science* **1994**, *265*, 1217–1219. [[CrossRef](#)] [[PubMed](#)]
41. Lietti, L.; Forzatti, P.; Berti, F. Role of the redox properties in the SCR of  $NO$  by  $NH_3$  over  $V_2O_5$ - $WO_3$ / $TiO_2$  catalyst. *Catal. Lett.* **1996**, *41*, 35–39. [[CrossRef](#)]
42. Geng, Y.; Huang, H.; Chen, X.; Ding, H.; Yang, S.; Liu, F.; Shan, W. The effect of Ce on a high-efficiency  $CeO_2$ / $WO_3$ - $TiO_2$  catalyst for the selective catalytic reduction of  $NO_x$  with  $NH_3$ . *RSC Adv.* **2016**, *6*, 64803–64810. [[CrossRef](#)]
43. Liu, F.; He, H. Structure-activity relationship of iron titanate catalysts in the selective catalytic reduction of  $NO_x$  with  $NH_3$ . *J. Phys. Chem. C* **2010**, *114*, 16929–16936. [[CrossRef](#)]
44. Bêche, E.; Charvin, P.; Perarnau, D.; Abanades, S.; Flamant, G. Ce 3d XPS investigation of cerium oxides and mixed cerium oxide ( $Ce_xTi_yO_z$ ). *Surf. Interface Anal.* **2008**, *40*, 264–267. [[CrossRef](#)]
45. Liu, C.; Chen, L.; Chang, H.; Ma, L.; Peng, Y.; Arandiyán, H.; Li, J. Characterization of  $CeO_2$ - $WO_3$  catalysts prepared by different methods for selective catalytic reduction of  $NO_x$  with  $NH_3$ . *Catal. Commun.* **2013**, *40*, 145–148. [[CrossRef](#)]
46. Shan, W.; Liu, F.; He, H.; Shi, X.; Zhang, C. An environmentally-benign  $CeO_2$ - $TiO_2$  catalyst for the selective catalytic reduction of  $NO_x$  with  $NH_3$  in simulated diesel exhaust. *Catal. Today* **2012**, *184*, 160–165. [[CrossRef](#)]



© 2018 by the authors. Licensee MDPI, Basel, Switzerland. This article is an open access article distributed under the terms and conditions of the Creative Commons Attribution (CC BY) license (<http://creativecommons.org/licenses/by/4.0/>).